JOURNAL OF CATALYSIS 157, 698–705 (1995)

Sulfidation Study of Molybdenum Oxide Using $MoO_3/SiO_2/Si(100)$ Model Catalysts and Mo_3^{IV}–Sulfur Cluster Compounds

J. C. Muijsers,* Th. Weber, *[1] R. M. van Hardeveld,* H. W. Zandbergen,† and J. W. Niemantsverdriet*[2]

*Schuit Institute of Catalysis, Eindhoven University of Technology, P.O. Box 513, 5600 MB Eindhoven, The Netherlands; and †National Centre for High Resolution Electron Microscopy, Delft University of Technology, Rotterdamseweg 137, 2628 AL Delft, The Netherlands

Received May 1, 1995; revised August 10, 1995

Monochromatic XPS spectra of the temperature-dependent sulfidation of $MoO_3/SiO_2/Si(100)$ model catalysts are compared with spectra of Mo–S cluster compounds in particular with those of $(NH_4)_2[Mo_3S_{13}]\cdot H_2O$ and its thermal decomposition products. XPS is used to identify different states of sulfur and molybdenum occurring during sulfidation. The spectra show the presence of bridging disulfide ligands and of substantial amounts of Mo^V in an early stage of the sulfidation. These findings suggest that the initial reaction of the MoO_3-type precursor with the H_2S/H_2 atmosphere consists of two elementary steps, namely an O–S exchange followed by an Mo–S redox process. © 1995 Academic Press, Inc.

1. INTRODUCTION

Hydrodesulfurization with MoS_2-based catalysts is a process of increasing importance and is applied in refineries all over the world. Several open questions concerning the preparation and the structure of the catalyst exist. In particular, the mechanism of the sulfidation reaction where the oxidic, MoO_3-type precursor is converted into the active MoS_2 phase is still under debate (1–4). Surface science techniques such as monochromatic X-ray photoelectron spectroscopy (XPS) can in principle reveal highly useful information on the states of both molybdenum and sulfur. However, the presence of porous, electrically insulating oxide supports generally leads to serious loss of spectral resolution, implying that a lot of potentially interesting XPS information cannot be obtained from technical HDS catalysts.

Model catalysts prepared on thin oxide films as the support offer much better opportunities for surface spectroscopies that utilize charged particles, such as XPS and SIMS (5–9). Articles from Spevack and McIntyre (6), Hayden and Dumesic (7), as well as from our own group (5) demonstrated the feasibility of this approach in studies on the sulfidation of molybdenum model catalysts. The results of de Jong *et al.* (5) gave evidence for the appearance of S_2^{2-} ligands in intermediate stages of the sulfidation process.

In this study we apply monochromatic XPS to follow the stepwise sulfidation of a $MoO_3/SiO_2/Si(100)$ model catalyst. To interpret the sulfur XPS spectra of the model catalyst, reference data of different kinds of sulfur ligands are needed. For this purpose we used the $(NH_4)_2[Mo_3S_{13}]\cdot H_2O$, $(NEt_4)_2[Mo_3S_7Cl_6]\cdot HCl$ (Et = C_2H_5) and $K_5[Mo_3S_4(CN)_9]\cdot 3KCN\cdot 4H_2O$ cluster compounds (Structures 1A–1C), which contain sulfide (S^{2-}) and disulfide (S_2^{2-}) ligands in different types of coordination. The most suitable compound for our purpose is $(NH_4)_2[Mo_3S_{13}]\cdot H_2O$, since the only ligands of molybdenum are sulfur. The anion (Structure 1A) contains three bridging and three terminal S_2^{2-} ligands as well as one central (apical) S^{2-} ligand. The compound $(NH_4)_2[Mo_3S_{13}]\cdot H_2O$ decomposes via well-documented steps to microcrystalline MoS_2 (10), yielding valuable information on the reactivity of sulfur ligands.

All compounds provide useful XPS references for the states of sulfur. Comparison of the XPS data of the partially sulfided $MoO_3/SiO_2/Si(100)$ model catalysts with those of the cluster compounds has led us to propose elementary reaction steps for the early stage of the sulfidation of molybdenum oxide catalysts.

2. EXPERIMENTAL

The compounds $(NH_4)_2[Mo_3S_{13}]\cdot H_2O$ (11), $(NEt_4)_2[Mo_3S_7Cl_6]\cdot HCl$ (12), and $K_5[Mo_3S_4(CN)_9]\cdot 3KCN\cdot 4H_2O$ (13) were prepared as described in the literature. Dilute solutions of $(NH_4)_2[Mo_3S_{13}]\cdot H_2O$ and $(NEt_4)_2[Mo_3S_7Cl_6]\cdot HCl$ in dimethylformamide (approximately 5 mg/ml) were prepared and several droplets were left to dry on the aluminum sample holders of the XPS spectrometer. Thermal decomposition experiments with

[1] Current address: Laboratories of Technical Chemistry, Swiss Federal Institute of Technology (ETH), CH-8092 Zürich, Switzerland.

[2] To whom correspondence should be addressed.

0021-9517/95 $12.00

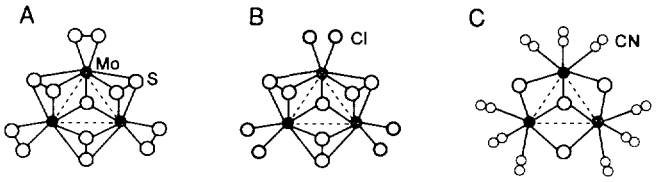

STRUCTURE 1

$(NH_4)_2[Mo_3S_{13}] \cdot H_2O$ were performed by heating the sample on the aluminum sample holder in a quartz tube reactor in an N_2 gas flow. A heating rate of 10°C/min was applied and the reactor was kept isothermal for 15 min at 260°C, 5 min at 310°C, or 240 min at 400°C to obtain the intermediate and final decomposition products. $K_5[Mo_3S_4(CN)_9] \cdot 3KCN \cdot 4H_2O$ was ground and pressed in indium foil in a glove box for the purpose of XPS measurements.

The $MoO_2/SiO_2/Si(100)$ model catalysts were prepared as follows. First silicon wafers with a (100) surface orientation were oxidized in air at 500°C for 24 h. This results in a relatively flat oxide layer with a thickness up to about 5 nm (14). Next, a thin layer of molybdenum oxide was deposited from a MoO_2Cl_2 solution of 5 g/liter MoO_2Cl_2 in ethanol, by spincoating the wafer in a dry nitrogen atmosphere at a rotation speed of 2800 rpm. No chloride was detected by XPS, indicating that MoO_2Cl_2 fully hydrolyzes to, presumably, a hydrated form of MoO_3 when exposed to air. The amount of deposited material was estimated as described by van Hardeveld *et al.* (15) to be 5.8×10^{15} (±10%) Mo atoms/cm^2. RBS measurements revealed a molybdenum loading of 5.7×10^{15} (±12%) atoms/cm^2. Sulfidation experiments were performed in a quartz tube reactor at 1 bar pressure and a flow rate of 50 ml/min. The catalysts were heated in 10% H_2S in H_2 with 5 K/min and kept isothermal at the desired temperature for 3 h.

XPS Spectra were obtained using a VG ESCALAB MK II spectrometer equipped with a monochromatic Al$K\alpha$ X-ray source and a hemispherical analyzer with a five-channel detector. During measurement the base pressure of the system was around 5×10^{-10} mbar. Spectra were recorded with a constant pass energy of 20 eV, unless stated otherwise. Binding energies were determined by computer fitting the measured spectra. Sample charging in the spectra of the cluster compounds was corrected for by reference to the C 1*s* peak at 284.6 eV. The binding energies are estimated to be accurate within 0.2 eV unless stated otherwise. Charging of the model catalyst in intermediate stages of sulfidation, typically a few tenths of an electron volt, could not be corrected for, except for the spectrum of the MoO_3 precursor, which was referenced to C 1*s* at 284.6 eV. The reason is that the layered geometry of the samples implies that charging, although limited, is a function of depth, while the C 1*s* peak refers mainly to the outer layer. As the precursor consists of an insulating oxidic phase, which is gradually, from the outside inward, converted to a semiconducting MoS_2 phase, charging becomes less with increasing degree of sulfidation. As a result the binding energies in spectra of samples in intermediate stages of sulfidation are accurate within approximately 0.4 eV only.

Samples that were treated in a reactor were always unloaded in a N_2-filled glove box (typically below 2 ppm H_2O and 1 ppm O_2) and transported to the XPS spectrometer in a standard transfer vessel under N_2, to prevent contact with air.

Two additional model catalysts, an oxidic and a fully sulfided one, were prepared under slightly different conditions for TEM analysis. A $MoO_3/SiO_2/Si(100)$ catalyst was prepared by spincoating with a solution of MoO_2Cl_2 in ethanol (10 g/liter) whereas the $MoS_2/SiO_2/Si(100)$ was prepared by spincoating with 10 g/liter in butanol solution and subsequent sulfiding at 400°C for 3 h. This resulted in relatively thick layers of MoO_3 and MoS_2 on thin, 2- to 3-nm-thick silicon oxide layers. TEM samples were prepared in air by the small-angle cleavage technique described in the literature (16). This relatively new technique, developed for semiconductors, allows high-resolution cross-sectional analysis of the model catalysts without the obscuring artifacts produced by ion milling, the traditional sample preparation technique. Samples prepared in this way were mounted on a copper grid, providing an electron transparent tip. Cross-sectional TEM (XTEM) micrographs were taken using a Philips CM30 ST FEG electron microscope (point resolution 0.2 nm, Fig. 3 top) or a Philips CM30T electron microscope (point resolution 0.24 nm, Fig. 3 bottom). Both microscopes were operated at 300 keV.

3. RESULTS

Molybdenum–Sulfur Compounds

Figure 1 shows the XPS spectra of the $(NH_4)_2[Mo_3S_{13}] \cdot H_2O$ compound and of its thermal decomposition products. The Mo 3*d* spectra of $(NH_4)_2[Mo_3S_{13}] \cdot H_2O$, of the intermediate decomposition products, and of the finally formed MoS_2 all contain the Mo $3d_{5/2}$ signal at a binding energy of 229.0 eV. This value is characteristic for molybdenum sulfur compounds with the metal in a formal oxidation state of 4+ (see Ref. (5) and literature cited therein). The broad S 2*s* peak on the low-binding-energy side of the Mo 3*d* doublet, however, changes definitely during the decomposition. These changes are more clearly revealed in the S 2*p* spectra, which are also included in Fig. 1.

The number and nature of the sulfur ligands change during the stepwise thermal decomposition of $(NH_4)_2[Mo_3S_{13}] \cdot H_2O$ to MoS_2. After the loss of water of crystallization around 150°C, the NH_4^+ cations react with the apical S^{2-} around 260°C, releasing NH_3 and H_2S (10).

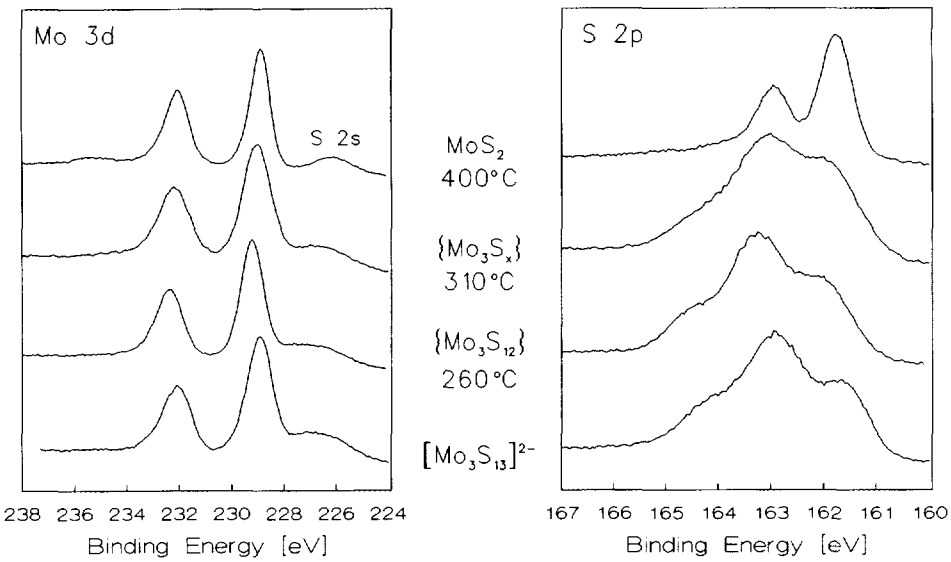

FIG. 1. Monochromatic Mo 3*d* and S 2*p* XPS spectra of $(NH_4)_2[Mo_3S_{13}] \cdot H_2O$ and its decomposition products.

As $(NH_4)_2[Mo_3S_{13}] \cdot H_2O$ contains three types of sulfur ligands, and the $\{Mo_3S_{12}\}$ decomposition intermediate only two, we start by analyzing the latter. The S 2*p* envelope fits well using two S 2*p* doublets of equal intensity, with S $2p_{3/2}$ binding energies at 163.1 and 161.8 eV, respectively. We attribute the S $2p_{3/2}$ at higher binding energy to the bridging S_2^{2-} ligands and the one at lower binding energy to terminal S_2^{2-} ligands. This implies that the negative charge on the terminal S_2^{2-} ligands is significantly higher than that on the bridging ones. This is in agreement with the result of an SCF-X_α-SW calculation (17) and can also be rationalized from the chemical behavior; the bridging S_2 entities are selectively attacked by nucleophilic agents and correspondingly the terminal ones by electrophilic agents (18). We thus conclude that the S 2*p* binding energy of bridging S_2^{2-} equals 163.1 ± 0.2 eV, and that of terminal S_2^{2-} is 161.8 ± 0.2 eV.

An estimate can be made for the binding energy of the apical S^{2-} by subtracting the S 2*p* spectrum of the $\{Mo_3S_{12}\}$ decomposition intermediate formed at 260°C from the spectrum of $(NH_4)_2[Mo_3S_{13}] \cdot H_2O$. This procedure results in a third S 2*p* doublet with an S $2p_{3/2}$ binding energy of 163.0 ± 0.5 eV for the apical sulfur.

The next decomposition step takes place at about 310°C and corresponds to the release of six equivalents of neutral sulfur from the three terminal S_2^{2-} ligands, in a reductive elimination reaction: $(Mo^{IV}\text{–}S_2^{2-} \rightarrow Mo^{IV} + S_2^0 + 2e)$. Simultaneously the bridging S_2^{2-} ligands are reduced to S^{2-} ligands $(S_2^{2-} + 2e \rightarrow 2S^{2-})$ forming an $\{Mo_3S_6\}$ intermediate, which is coordinatively unsaturated and tends to aggregate to microcrystalline MoS_2 (10). The corresponding spectrum in Fig. 1 still shows the presence of bridging S_2^{2-} ligands, indicating that the conditions employed, i.e., heating to 310°C for 5 min, does not yet convert all $\{Mo_3S_{12}\}$ in this state. Prolonged heating of the compound at 400°C leads to the top spectrum shown in Fig. 1. The single S 2*p* doublet has an S $2p_{3/2}$ binding energy of 161.8 eV, in agreement with the value known from literature for MoS_2 (19).

The XPS spectra of the $(NEt_4)_2[Mo_3S_7Cl_6] \cdot HCl$ and $K_5[Mo_3S_4(CN)_9] \cdot 3KCN \cdot 4H_2$) cluster compounds are shown in Fig. 2. Although charging seriously degrades the quality of the $(NEt_4)_2[Mo_3S_7Cl_6] \cdot HCl$ spectra, the binding energies of the Mo 3*d* and the S 2*p* doublets (229.1 and 162.8 eV, respectively) can be determined with sufficient accuracy to confirm that the bridging S_2^{2-} ligands of the $(NH_4)_2[Mo_3S_{13}] \cdot H_2O$ compound possess the higher binding energy among the two disulfide ligands. The spectrum of $K_5[Mo_3S_4(CN)_9] \cdot 3KCN \cdot 4H_2O$ provides a S 2*p* binding energy of 161.6 eV for the μ_2-S^{2-} ligands. Apparently, these have approximately the same binding energy as the basal plane μ_3-S^{2-} ligands of MoS_2. The Mo 3*d* binding energy of 229.3 eV again corresponds to molybdenum in a formal 4+ state.

All S $2p_{3/2}$ binding energies are summarized in Table 1. Note that terminal S_2^{2-} ligands and the basal plane μ_3-S^{2-} in MoS_2 cannot be distinguished on the basis of their XPS spectra, which is important for the interpretation of XPS spectra of sulfided molybdenum catalysts.

Model Catalyst

Figure 3 shows transmission electron micrographs of two model catalysts, one oxidic and the other after sulfidation

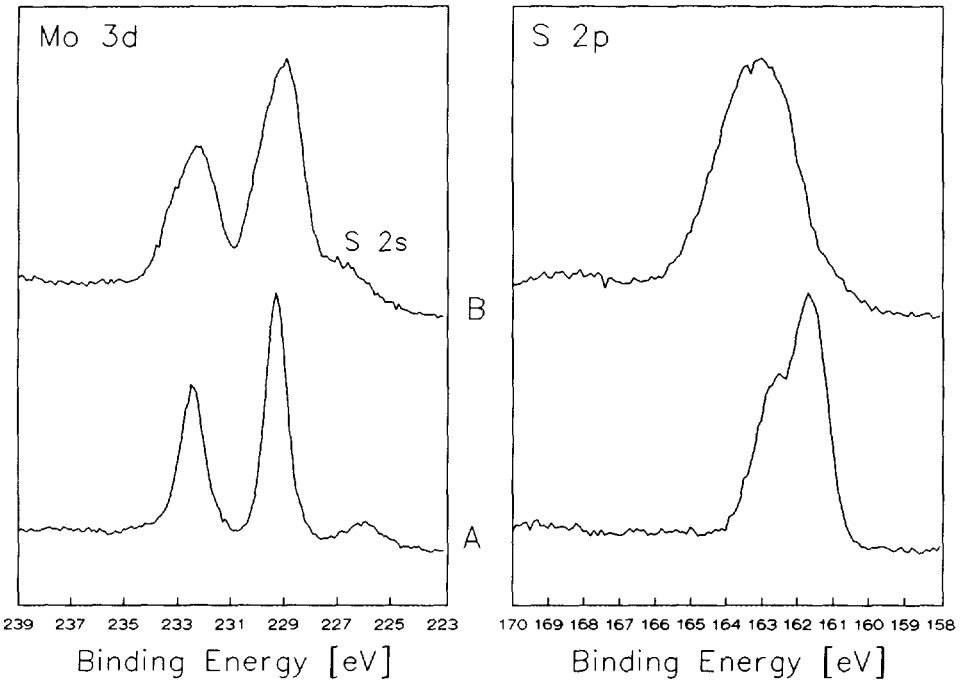

FIG. 2. Mo 3*d* and S 2*p* XPS spectra of (A) $K_5[Mo_3S_4(CN)_9] \cdot 3KCN \cdot 4H_2O$ and (B) $(NEt_4)_2[Mo_3S_7Cl_6] \cdot HCl$.

in H_2S/H_2 at 400°C, for 3 h. The TEM micrograph of the freshly prepared, oxidic $MoO_3/SiO_2/Si(100)$ model catalyst in Fig. 3 (top) shows two amorphous layers on top of the silicon crystal. Note that the distinction between the outer layer, MoO_3, which is approximately 3 nm thick, and the approximately 2.5-nm SiO_2 layer is clearly visible. Although the TEM image represents only a very small portion of the model catalyst, it indicates that the MoO_3 phase forms a flat layer of homogeneous thickness on the $SiO_2/Si(100)$ model support.

Sulfidation leads to the formation of a microcrystalline MoS_2 phase containing randomly oriented stacks of slabs (Fig. 3 (bottom)). The absence of a preferred orientation indicates that there is little or no chemical interaction with the supporting SiO_2 layer. Note that the Mo loading of this model catalyst was higher than the one used for Fig. 3 (top); the thickness of the MoS_2 layer is approximately 6 nm. The images of Fig. 3 illustrate that the small-angle cleaving technique produces samples that are well suited for TEM analysis, although we should mention that quite some experience is required to have a reasonable success rate.

TABLE 1

XPS S $2p_{3/2}$ Binding Energies of Mo–S and S Reference Compounds

Compound	Type of S ligand	Binding energy (eV)
$(NH_4)_2[Mo_3S_{13}] \cdot H_2O$	S_2^{2-} terminal	161.8
	S_2^{2-} bridging	163.1
	S^{2-} apical	163.0 ± 0.5
MoS_2	μ_3-S^{2-}	161.8
$(NEt_4)_2[Mo_3S_7Cl_6] \cdot HCl$	S_2^{2-} bridging	162.8
$K_5[Mo_3S_4(CN)_9] \cdot 3KCN \cdot 4H_2O$	μ_2-S^{2-}	161.6
Elemental sulfur, S_8[a]	S^0	164.0

[a] Reference (5).

The monochromatic XPS spectra of the $MoO_3/SiO_2/Si(100)$ model catalyst in Fig. 4 show the effect of sulfidation as a function of temperature. Owing to the sufficiently conducting model support and the use of a monochromated source, the different states in the Mo 3*d* and the S 2*p* regions can well be identified and also the S 2*s* peak on the low-binding-energy side of the Mo 3*d* doublet is almost entirely resolved. Although sulfidation at room temperature already has a considerable effect, the fully sulfided state appears to be reached between 250 and 300°C. Several intermediate situations emerge as well. We first describe the spectra of the limiting cases.

The Mo 3*d* spectrum of the oxidic precursor consists of a single Mo 3*d* doublet with a Mo $3d_{5/2}$ binding energy of 232.6 eV. This value, although characteristic of molybdenum with a formal charge of 6+ in an oxidic surrounding, is slightly higher than that of crystalline MoO_3, 232.3 eV (20), but agrees well with the binding energy of

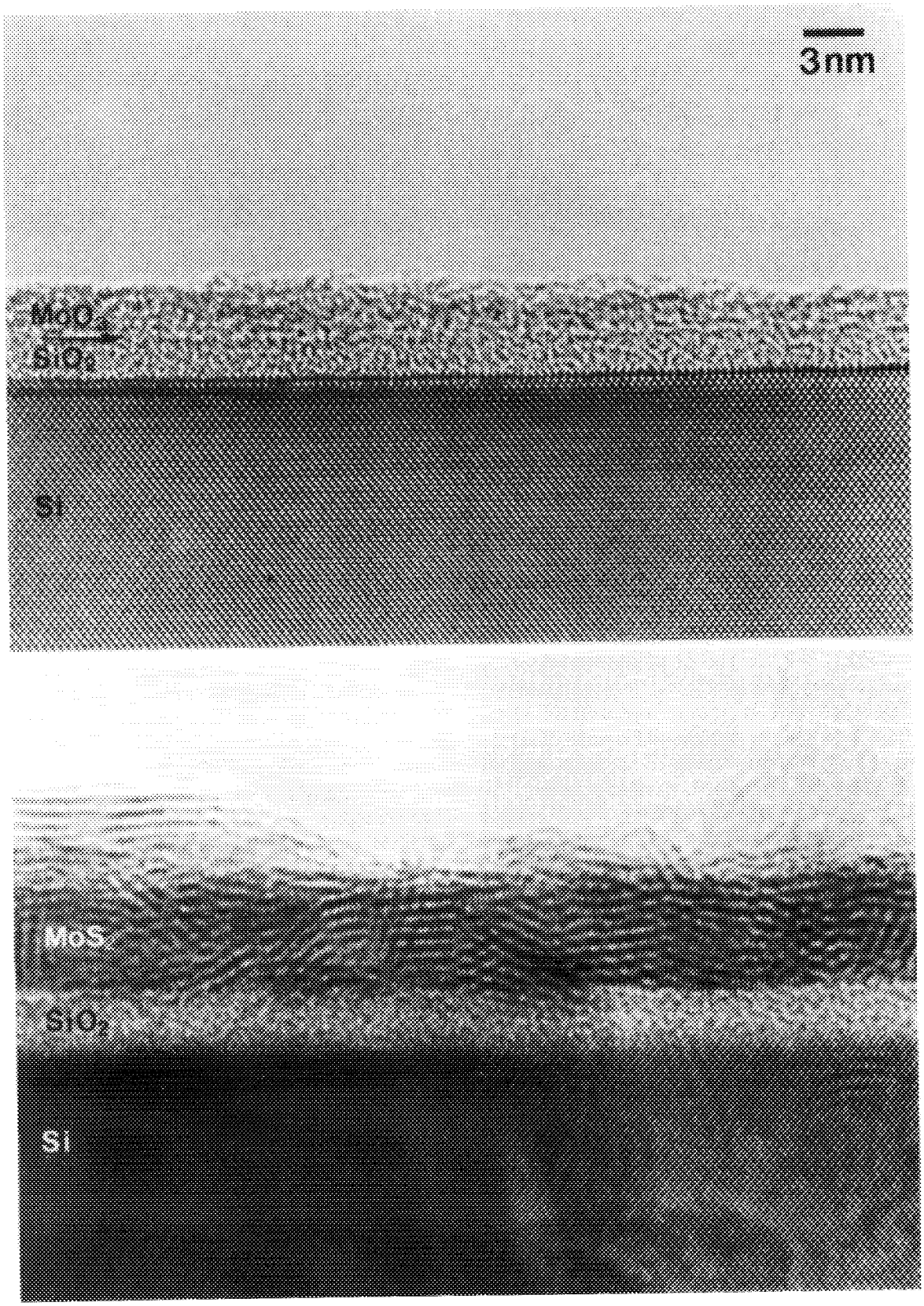

FIG. 3. TEM micrographs of $MoO_3/SiO_2/Si(100)$ (top, the MoO_3/SiO_2 interface is indicated by an arrow) and $MoS_2/SiO_2/Si(100)$ (bottom).

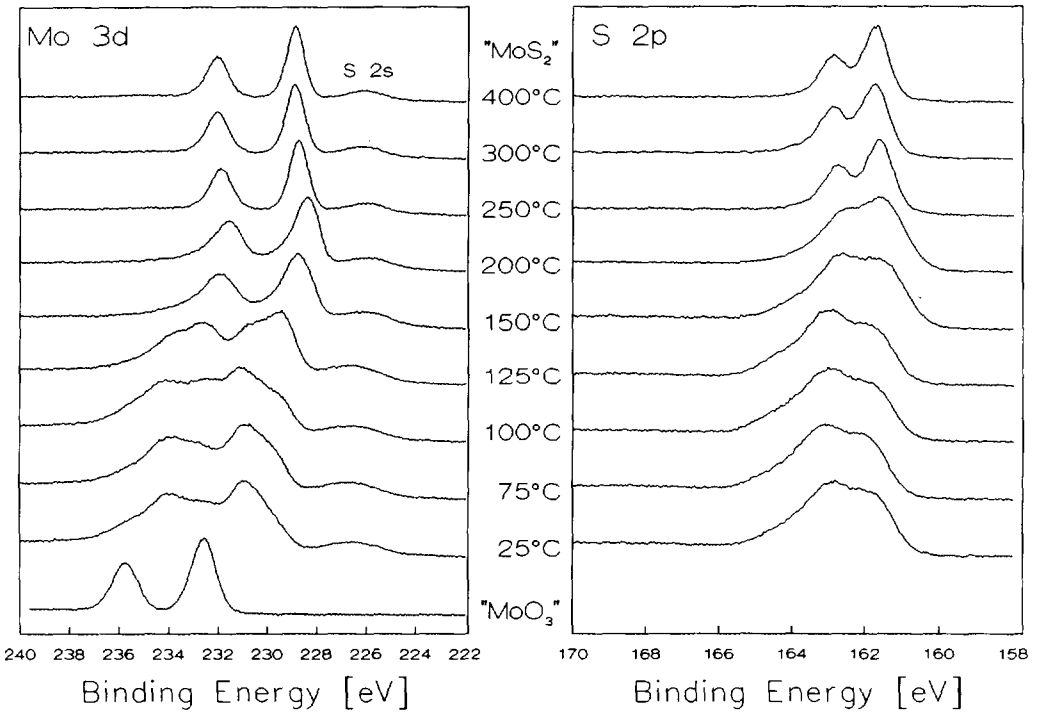

FIG. 4. Mo 3*d* and S 2 *p* XPS spectra of the $MoO_3/SiO_2/Si(100)$ model catalyst sulfided at the temperatures indicated.

$MoO_3 \cdot H_2O$, which equals 232.6 eV (20). As the MoO_3 phase on the model support prepared by hydrolysis of MoO_2Cl_2 was not calcined, the presence of a hydrated form of MoO_3 seems plausible.

The Mo 3*d* doublet observed for the model catalyst sulfided at 400°C has a Mo $3d_{5/2}$ binding energy of 229.0 eV, which is typical for molybdenum with a formal charge state of 4+ as in MoS_2. The S 2*p* spectrum of the sample consists of a single doublet with a S $2p_{3/2}$ binding energy of 161.7 eV, consistent with the S^{2-}-type ligands present in MoS_2, although terminal S_2^{2-} would appear at the same value. The presence of the latter can therefore not be excluded.

The Mo 3*d* spectra of the catalysts sulfided at intermediate temperatures can all be interpreted in terms of the Mo^{6+} and Mo^{4+} doublets described above and one additional doublet with a Mo $3d_{5/2}$ binding energy of 230.8 eV. This doublet, already present after sufidation at room temperature, can be assigned to molybdenum having a formal charge of 5+, possibly in an oxysulfidic surrounding. The contribution of Mo^{6+} disappears from the spectra of samples sulfided at 150°C and higher, while the Mo^{4+} starts to form in substantial amounts at sulfidation temperatures above 75°C.

All S 2*p* spectra can be fitted with two S 2*p* doublets, having binding energy values for the S $2p_{3/2}$ peak at 161.7 and 162.9 eV. In the S 2*p* XPS spectra of the model catalyst sulfided at room temperature we find both S 2*p* doublets. Keeping in mind the S $2p_{3/2}$ values found for the different sulfur ligands in $(NH_4)_2[Mo_3S_{13}] \cdot H_2O$, we can assign the 162.9 eV S $2p_{3/2}$ peak to bridging S_2^{2-} ligands and the 161.7 eV S $2p_{3/2}$ peak to terminal S_2^{2-} and/or S^{2-} ligands. We conclude that bridging S_2^{2-} species are clearly present after sulfidation at low temperatures, but disappear almost completely above 200–250°C. We cannot exclude on the basis of XPS that terminal S_2^{2-} ligands exist at these temperatures.

Finally, we note that the O 1*s* signal attributable to the molybdenum oxide and oxysulfide phases disappears from the spectra of samples sulfided at 300°C and higher. This confirms that the experimental procedure that involves the unloading of the model catalyst from the sulfidation reactor in a glove box and the subsequent transportation under nitrogen to the XPS spectrometer is a legitimate one.

4. DISCUSSION

The XPS results of Fig. 4 reveal in detail how the states of molybdenum and sulfur change during temperature-programmed sulfidation. Molybdenum is initially present in the 6+ state but converts through a Mo^{5+} intermediate to the eventual Mo^{4+} present in MoS_2. Sulfur can be present in at least two, but possibly more states. Unfortunately, the measurements on the Mo_3 cluster compounds indicate that XPS does not distinguish between terminal S_2^{2-} and S^{2-}, and hence a more detailed identification is not possible.

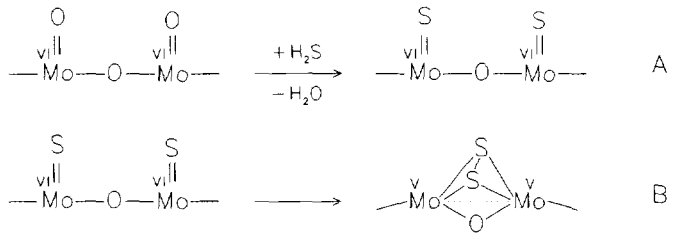

FIG. 5. Schematic representation of the initial reaction steps in the sulfidation of our $MoO_3/SiO_2/Si(100)$ model catalyst.

Nevertheless, the S 2*p* spectra do indicate that bridging S_2^{2-} groups appear at sulfidation temperatures up to 200°C, while eventually the sulfide ligands account for most of the sulfur present in the catalyst.

We suggest the following global reaction mechanism. The first step (see reaction A in Fig. 5) is an oxygen sulfur exchange at the surface of the oxidic catalyst precursor with H_2S from the gas phase, resulting in S^{2-} ligands bonded to Mo^{VI} centers. This reaction, which has been postulated by others as well (21, 22), takes place at room temperature already. If the precursor consisted of crystalline MoO_3, the terminally bonded oxygen atoms of the octahedrally coordinated Mo centers would be the first to exchange. However, we do not expect that the catalyst precursor contains crystalline MoO_3; in fact the TEM image of Fig. 3 indicates that the molybdenum oxide is amorphous. Due to its preparation by hydrolysis of MoO_2Cl_2 according to

$$MoO_2Cl_2 + 2H_2O \rightarrow MoO_2(OH)_2 + 2HCl$$
$$MoO_2(OH)_2 \rightarrow MoO_3 \cdot H_2O,$$

the local structure of the freshly prepared catalyst is probably closer to that of α-$MoO_3 \cdot H_2O$ (23) and $MoO_3 \cdot 2H_2O$ (24). We expect H_2O and/or OH^- ligands to be present at positions where in crystalline MoO_3 only O^{2-} ligands occur. This makes the structure of our catalyst precursor much less compact and as a result a reaction with H_2S is much easier such that sulfidation may take place at room temperature already. Independent of any particular structural property, the formation or the release of water provides the thermodynamic driving force. We thus propose reaction A depicted in Fig. 5.

The S 2*p* spectra of Fig. 4 indicate that a considerable fraction of the sulfur in the catalyst sulfided at 25°C is the bridging S_2^{2-} ligand. We need to explain how bridging S_2^{2-} ligands arise on the catalyst surface if we only offer S^{2-} in the form of H_2S in the gas atmosphere.

The oxidation of S^{2-} to S_2^{2-} can only have occurred in the coordination sphere of the molybdenum. We therefore propose that the initial O–S exchange is followed by a redox reaction between two adjacent $Mo^{VI}{=}S_t^{2-}$ fragments (see reaction B in Fig. 5), resulting in the formation of a bridging S_2^{2-} ligand and the reduction of molybdenum. The formation of disulfide ligands during sulfidation is also observed with Raman spectroscopy by other authors (25, 26). The Mo 3*d* XPS spectrum of the catalysts sulfided at room temperature indicates that Mo^{VI} is reduced to Mo^{V} mainly. However, the XPS spectrum also indicates small amounts of Mo^{IV}. They can be formed from $Mo^{VI}(=S_t^{2-})_2$ fragments by conversion in analogy to reaction B in Fig. 5, to a terminal S_2^{2-} ligand at a Mo^{IV} center.

In a further stage of the sulfidation process reductive elimination of terminal S_2^{2-} ligands accompanied by the reduction of bridging S_2^{2-} ligands takes place in reactions that also occur during the decomposition of $(NH_4)_2[Mo_3S_{13}] \cdot H_2O$, as discussed in connection with Fig. 1. The released sulfur is expected to react in part with H_2 to H_2S.

All reaction steps described above are in agreement with the results presented in Fig. 4 as well as with more recent results on model catalyst with lower Mo loading, which will be published elsewhere (27). Due to the abundantly present S_2^{2-} ligands, the mechanism accounts for S/Mo ratios in excess of two as have been reported in intermediate stages of sulfidation (5, 22, 26, 28), while it also explains the evolution of H_2S observed in temperature-programmed sulfidation studies by Moulijn and co-workers (21). We repeat, however, that our results are representative of MoO_3 catalysts on a silica model support that have *not* been calcined and are expected to contain $MoO_3 \cdot xH_2O$ phases. In a subsequent paper (27) we show that precalcined catalysts sulfide at a low rate and via a slightly different mechanism.

The XPS spectra of the inorganic cluster compounds of Figs. 1 and 2 have been essential in establishing the S 2*p* binding energies of various types of sulfur ligands as compiled in Table 1. Although the use of monochromatic XPS in combination with an electrically conducting thin film support allows for identification of several of these sulfur states in sulfided model catalysts, it is unfortunate that terminal S_2^{2-} and S^{2-} appear to have similar binding energies. This implies that based on XPS spectra alone the presence of terminal S_2^{2-} ligands in a sulfided MoS_2 catalyst cannot be excluded. Their presence, however, is unlikely because terminal S_2^{2-} ligands, if present on edges of metal centers of MoS_2 particles, are expected to undergo reductive elimination reactions. Formation of reduced, coordinatively unsaturated Mo centers is known to occur in hydrogen atmospheres (29, 30).

The aim of this study was to gain qualitative information on the sulfidation process. Quantification is impeded by the relatively high molybdenum loading of about 6×10^{15} Mo/cm^2, which corresponds to several layers. Consequently, sulfidation, particularly at lower temperatures, resulted in concentration gradients in the molybdenum layer

(see also Ref. (5)) that makes quantification in terms of Mo : O : S stoichiometries difficult. Experiments with angle-dependent XPS showed that after 3 h of H_2S/H_2 treatment at 100°C the sulfidation at the surface was in a significantly further stage than at deeper layers. Thus, experiments on model catalysts with lower molybdenum oxide loadings (i.e., on the order of a monolayer) allow for quantitative conclusions from the XPS spectra. Such studies, which also address the effect of calcination and water on the sulfidation of MoO_3, are presently in progress and will be reported soon (27, 31).

ACKNOWLEDGMENTS

We are indebted to Dr. V. H. J. de Beer and his co-workers for fruitful collaborations. Valuable discussions with Dr. V. H. J. de Beer and Professors J. A. R. van Veen and J. A. Moulijn are gratefully acknowledged. We thank Dr. L. J. van IJzendoorn for the RBS measurements. This work was supported by Grant PGS 70-154 from the Netherlands Organization for Scientific Research.

REFERENCES

1. Prins, R., de Beer, V. H. J., and Somorjai, G. A., *Catal. Rev.-Sci. Eng.* **31,** 1 (1989).
2. Topsøe, H., Clausen, B. S., Topsøe, N.-Y., and Zeuthen, P., *in* "Catalysis in Petroleum Refining, Proc. Conf. on Catalysts in Petroleum Refining 1989" (D. L. Trimm, S. Akashah, M. Absi Halabi, and A. Bishara, Eds.), p. 77. Elsevier, Amsterdam, 1990.
3. Knözinger, H., *in* "Proceedings, 9th International Congress on Catalysis, Calgary, 1988" (M. J. Phillips and M. Ternan, Eds.), Vol. 5, p. 20. Chem. Institute of Canada, Ottawa, 1988.
4. Scheffer, B., Arnoldy, P., and Moulijn, J. A., *J. Catal.* **112,** 516 (1988).
5. de Jong, A. M., Borg, H. J., van IJzendoorn, L. J., Soudant, V. G. F. M., de Beer, V. H. J., van Veen, J. A. R., and Niemantsverdriet, J. W., *J. Phys. Chem.* **97,** 6477 (1993).
6. Spevack, P. A., and McIntyre, N. S., *J. Phys. Chem.* **97,** 11031 (1993).
7. Hayden, T. F., and Dumesic, J. A., *J. Catal.* **103,** 366 (1987).
8. Jiménez-González, A., and Schmeisser, D., *J. Catal.* **130,** 332 (1991).
9. Shild, Ch., Engweiler, J., Nickl, J., Baiker, A., Hund, M., Kilo, M., and Wokaun, A., *Catal. Lett.* **25,** 179 (1994).
10. Müller, A., and Diemann, E., *Chimia* **39,** 312 (1985).
11. Müller, A., and Krickemeyer, E., *Inorg. Synth.* **27,** 47 (1990).
12. Fedin, V. P., Sokolov, M. N., Mironov, Yu. V., Kolesov, B. A., Tkachev, S. V., and Fedorov, V. Ye., *Inorg. Chim. Acta* **167,** 39 (1990).
13. Müller, A., and Reinsch, U., *Angew. Chem.* **92,** 69 (1980).
14. Gunter, P. L. J., de Jong, A. M., Niemantsverdriet, J. W., and Reiter, H. J. H., *Surf. Interface Anal.* **19,** 161 (1992).
15. van Hardeveld, R. M., Gunter, P. L. J., van IJzendoorn, L. J., Wieldraaijer, W., Kuipers, E. W., and Niemantsverdriet, J. W., *Appl. Surf. Sci.*, **84,** 339 (1995).
16. McCaffrey, J. P., *in* "Specimen Preparation for Transmission Electron Microscopy of Materials III, Materials Research Society Symposium Proceedings" (R. Anderson, B. Tracy, and J. Bravman, Eds.), Vol. 254, p. 109. Materials Research Scoiety, Pittsburgh, 1992.
17. Müller, A., Wittenben, V., Krickemeyer, E., Bögge, H., and Lemke, H., *Z. Anorg. Allg. Chem.* **605,** 175 (1991).
18. Zimmermann, H., Hegetschweiler, K., Keller, T., Gramlich, V., Schmalle, H. W., Petter, W., and Schneider, W., *Inorg. Chem.* **30,** 4336 (1991).
19. Patterson, Th. A., Carver, J. C., Leyden, D. E., and Hercules, D. M., *J. Phys. Chem.* **80,** 1700 (1976).
20. Barr, T. L., *J. Phys. Chem.* **82,** 1801 (1978).
21. Arnoldy, P., van den Heijkant, J. A. M. de Bok, G. D., and Moulijn, J. A. *J. Catal.* **92,** 35 (1985).
22. de Boer, M., van Dillen, A. J. Koningsberger, D. C., and Geus, J. W., *J. Phys. Chem.* **98,** 7862 (1994).
23. Gmelin Handbook of Inorganic Chemistry, 8th ed., Molybdenum Supplement Vol. B3a, p. 33. Springer-Verlag, Berlin, 1986.
24. Gmelin Handbook of Inorganic Chemistry, 8th ed., Molybdenum Supplement Vol. B3a, p. 23. Springer-Verlag, Berlin, 1986.
25. Schrader, G. L., and Cheng, C. P., *J. Catal.* **80,** 369 (1983).
26. Payen, E., Kasztelan, S., Houssenby, S., Szymanski, R., and Grimblot, J., *J. Phys. Chem.* **93,** 6501 (1989).
27. Weber, Th., Muijsers, J. C., Handels, F. J. A., de Beer, V. H. J., van Veen, J. A. R., and Niemantsverdriet, J. W., to appear.
28. Weber, Th., Muijsers, J. C., and Niemantsverdriet, J. W., *J. Phys. Chem.* **99,** 9194 (1995).
29. Diemann, E., Weber, Th., and Müller, A., *J. Catal.* **148,** 288 (1994).
30. Müller, B., van Langeveld, A. D., Moulijn, J. A., and Knözinger, H., *J. Phys. Chem.* **97,** 9028 (1993).
31. Weber, Th., Muijsers, J. C., van Wolput, J. H. M. C., Verhagen, C. P. J., and Niemantsverdriet, J. W., to appear.